Journal of Magnetism and Magnetic Materials 473 (2019) 215–220

Contents lists available at ScienceDirect

Journal of Magnetism and Magnetic Materials

journal homepage: www.elsevier.com/locate/jmmm

Research articles

Disruption of amyloid aggregates by artificial ferritins

L. Balejčíková[a], V.I. Petrenko[b,c,*], M. Baťková[d], K. Šipošová[d], V.M. Garamus[e], L.A. Bulavin[c], M.V. Avdeev[b], L. Almásy[f,g], P. Kopčanský[d]

[a] Institute of Hydrology, Slovak Academy of Sciences, Dúbravská cesta 9, 841 04 Bratislava, Slovakia
[b] Joint Institute for Nuclear Research, Joliot-Curie Street 6, 141980 Dubna, Moscow Region, Russia
[c] Taras Shevchenko National University of Kyiv, Volodymyrska Street 64, 01033 Kyiv, Ukraine
[d] Institute of Experimental Physics, Slovak Academy of Sciences, Watsonova 47, 040 01 Kosice, Slovakia
[e] Helmholtz-Zentrum Geesthacht: Centre for Materials and Coastal Research, Max-Planck-Street 1, 21502 Geesthacht, Germany
[f] Institute for Solid State Physics and Optics, Wigner Research Centre for Physics, Hungarian Academy of Sciences, H-1525, Budapest POB 49, Hungary
[g] State Key Laboratory of Environment-Friendly Energy Materials, Southwest University of Science and Technology, Mianyang 621010, China

ARTICLE INFO

Keywords:
Amyloid aggregates
Magnetoferritin
Ferritin
Interactions between amyloid and magnetic materials
Anti-amyloid effect
Disruption of amyloid

ABSTRACT

Presence of protein amyloid aggregates is associated with many neurodegenerative disorders, such as Alzheimer's disease etc. The effect of magnetoferritin and reconstructed ferritin on the structure of lysozyme amyloid aggregates was studied using small-angle X-ray scattering, atomic force microscopy and thioflavin T fluorescence measurements. It has been shown that both magnetoferritin and reconstructed ferritin molecules affect the size, structure and amount of the amyloid fibrils. We assume that the anti-amyloid effect of magnetoferritin and reconstructed ferritin is due to the presence of iron in solutions but is not associated with the magnetic character of the iron oxide phases, i.e. magnetite/maghemite for magnetoferritin and ferrihydrite for ferritin.

1. Introduction

Unusual protein-protein interactions of normally soluble proteins that have undergone structural transitions result in the formation of intracellular and extracellular amyloid structures enriched in intermolecularly hydrogen bonded β-sheets. Abnormal protein aggregation and accumulation of formed fibrils are characteristic features for a range of, if not all, neurodegenerative disorders such as Alzheimer's, Huntington's, Parkinson's, as well as non-neuropathic amyloidosis including type II diabetes, familial amyloid polyneuropathy and polyglutamine disorders [1–3]. The exact mechanism of amyloid aggregates formation is not known despite intense research activities.

Lysozyme belongs to structurally diverse proteins that may aggregate into β-sheet-rich amyloid deposits. Moreover, lysozyme is one of the best characterized and most studied proteins with ability to form amyloid fibrils [4–7].

Nanoparticles (NPs), due to their size-dependent physical and chemical properties, have shown remarkable potential for a wide range of applications over the past decades. It should be noted that for the biomedical applications NPs must combine some characteristics of stability, biocompatibility, as well as specific localization at the biological target site. Magnetic NPs are being explored for their role in diagnosing, preventing, treating or even causing amyloid diseases. Previously it was shown that magnetic NPs can significantly affect the process of amyloidogenesis depending on their physicochemical characteristics such as size, charge, shape, and composition [8–11]. Also, Fe_3O_4-based nanoparticles are able to affect protein amyloid aggregation *in vitro* [12–14].

Magnetoferritin (MF) represents a synthetic macromolecule consisting of a native apoferritin hollow sphere and magnetic nanocrystals (Fe_3O_4, γ-Fe_2O_3) formed inside by controlled chemical process. The average number of iron atoms per apoferritin molecule, referred as iron loading or iron loading factor (LF) can be varied by modification of specific conditions during chemical synthesis [15,16]. The physical-chemical properties of magnetoferritin and reconstructed ferritin were investigated in details [15–30]. Studies of *in vitro* reconstruction of ferritin focused on the understanding of ferritin formation kinetics, autocatalytic function as well as the mechanisms of iron ions uptake, revealed that reconstructed ferritin contains iron core of ferrihydrite-like mineral surrounded by apoferritin [28–30]. Therefore, using magnetoferritin and reconstructed ferritin has the advantage that the iron content can be regulated by the synthesis conditions.

In our previous SAXS study of MFs with various LFs, we observed a partial destruction and polydispersity growth of MFs attributed to iron

* Corresponding author at: Joint Institute for Nuclear Research, Joliot-Curie Street 6, 141980 Dubna, Moscow Region, Russia.
E-mail address: vip@nf.jinr.ru (V.I. Petrenko).

https://doi.org/10.1016/j.jmmm.2018.10.055
Received 23 June 2018; Received in revised form 11 October 2018; Accepted 11 October 2018
Available online 12 October 2018
0304-8853/

binding into MF [26,27]. MF exhibits capability to reduce both the size and amount of lysozyme amyloid aggregates. Apoferritin, on the other hand, does not affect the lysozyme amyloid fibrils. This suggests that destruction activity of MF is related to its iron containing core [31].

In the present study, we investigated the effect of artificial ferritins on lysozyme amyloid fibrils using SAXS, atomic-force microscopy and fluorescence measurements. We compared the effect of different magnetic iron nanoparticles inside apoferritin shell on the stability of lysozyme amyloid aggregates. We observed that both, magnetoferritin and reconstructed ferritin affected the size, structure as well as the amount of lysozyme amyloid fibrils.

2. Materials and methods

2.1. Chemicals

3-[(1,1-dimethyl-2-hydroxyethyl)amino]-2-hydroxypropanesulfonic acid (AMPSO), 4-(2-hydroxyethyl)-1-piperazineethanesulfonic acid (HEPES), ammonium ferrous sulphate hexahydrate ($(NH_4)_2Fe(SO_4)_2{\cdot}6H_2O$), apoferritin from equine spleen (A3641/SLBD5084V), glycine, lysozyme from hen egg white (E.C. number: 3.2.1.17, lyophilized powder, L 6876, ~50,000 units mg^{-1} protein), H_2O_2, KSCN, NaOH and trimethylamine N-oxide were purchased from Sigma-Aldrich (St. Louis, MO; USA). Coomassie brilliant blue was obtained from Fluka. All other chemicals (ethanol, HCl, H_3PO_4) were of analytical grade.

2.2. Magnetoferritin and reconstructed ferritin synthesis

Magnetoferritin (MF) was prepared by the additions of ferrous ions into the empty protein shell of native apoferritin (NA) with a concentration of ~2 mg/mL. First, the NA solution was added into a 0.05 M AMPSO buffer with pH adjusted to pH 8.6 using 2 M NaOH solution, utilizing a pH meter (Mettler Toledo SevenEasy S20-KS) and pH electrode (Mettler Toledo Inlab®Science Pro). The reaction vessel with NA solution was hermetically closed. It should be noted that the demineralized water used for all solutions' preparation was deaerated using inert nitrogen for 1 h to provide anaerobic conditions and controlled oxidation. Ferrous ions source represented 0.1 M solution of Mohr's salt ((NH4)2Fe(SO4)2·6H2O) and an oxidant source, stoichiometric amount of 0.07 M solution of trimethylamine N-oxide. Synthesis was realized by the gradual addition of reactants in 10 steps over 100 min using syringes at 65 °C under constant stirring via a magnetic stirrer with heating (IKA C-MAG HS 7).

Reconstructed ferritin (RF) was prepared by the procedure analogue to MF synthesis. The difference was in the buffer composition, which was composed of 0.02 M HEPES adjusted by 2 M NaOH solution to a final pH value 7.4. The temperature was set to 37 °C.

MF and RF were freeze dried to obtain powders. First, liquid MF and RF were frozen at −20 °C for 8 h, followed by lyophilisation for 24 h.

The loading factors of MF and RF, LF, representing the average number of iron atoms per one apoferritin biomacromolecule, were determined spectrophotometrically [32].

2.3. Lysozyme amyloid fibrils preparation

Powder of lysozyme was dissolved in 0.2 M glycine-HCl buffer of pH 2.2 to a final concentration of 10 mg/ml. The pH value was controlled by the pH meter (Mettler Toledo SevenEasy S20-KS) and pH electrode (Mettler Toledo Inlab®Science Pro). Such prepared colloidal mixture of lysozyme also contained 80 mM NaCl solution. Then, lysozyme solution was mixed at 65 °C for 2 h under constant stirring via a magnetic stirrer with heating (IKA C-MAG HS 7) to prepare lysozyme amyloid fibrils (LA).

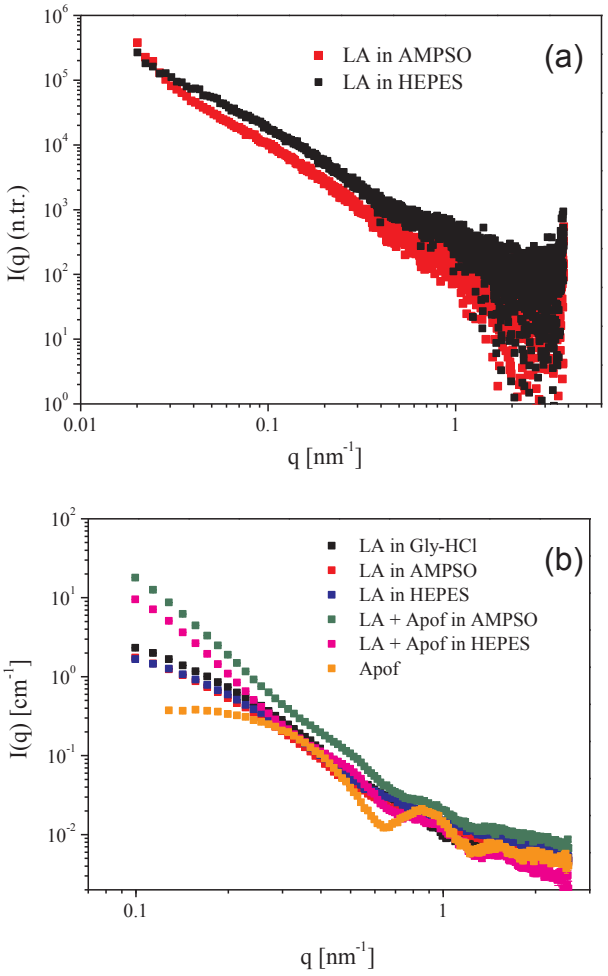

Fig. 1. (a) Scattering curves of lysozyme amyloid aggregates in AMPSO and HEPES buffer, measured on the P12 BioSAXS beamline. (b) Scattering curves of lysozyme amyloid aggregates dispersed in different buffers, apoferritin alone, as well as mixture of LA with apoferritin obtained using laboratory SAXS.

2.4. Sample preparation for study effects of magnetoferritin and reconstructed ferritin on lysozyme amyloid aggregates

MF and RF in powder form was diluted in AMPSO and HEPES, respectively, to achieve 100 mg/ml protein concentration. Subsequently, lysozyme fibril solutions (40 µl) were diluted in appropriate buffer (AMPSO buffer in the case of MF and HEPES for RF solutions) to concentration of 2 mg/ml in 200 µl. Before buffer addition to volume 200 µl, MF and RF were added to fibrils solutions in concentrations 1, 2, 4, 10 and 20 mg/ml, to achieve amyloid:ferritin weight ratios of 2:1, 1:1, 1:2, 1:5 and 1:10, followed by incubation at 37 °C for 24 h.

2.5. Small angle X-ray scattering

Small angle X-ray scattering measurements were performed using two instruments. First set of measurements was carried out on a laboratory SAXS instrument (Bruker AXS GmbH, Karlsruhe, Germany), equipped with a IµS micro-focus X-ray source with a power of 30 W and used Cu Kα radiation with wavelength of 0.154 nm (Incoatec, Geesthacht, Germany), and a VÅNTEC-2000 detector (14 × 14 cm^2 and 2048 × 2048 pixels). Distance between sample and detector was 108.3 cm and the accessible q ranged from 0.1 to 2.3 nm^{-1}. Samples were kept in quartz glass capillaries of 2 mm internal thickness. All measurements were carried out at 25 °C. The raw scattering data were corrected for the background from the solvent measured in capillary of

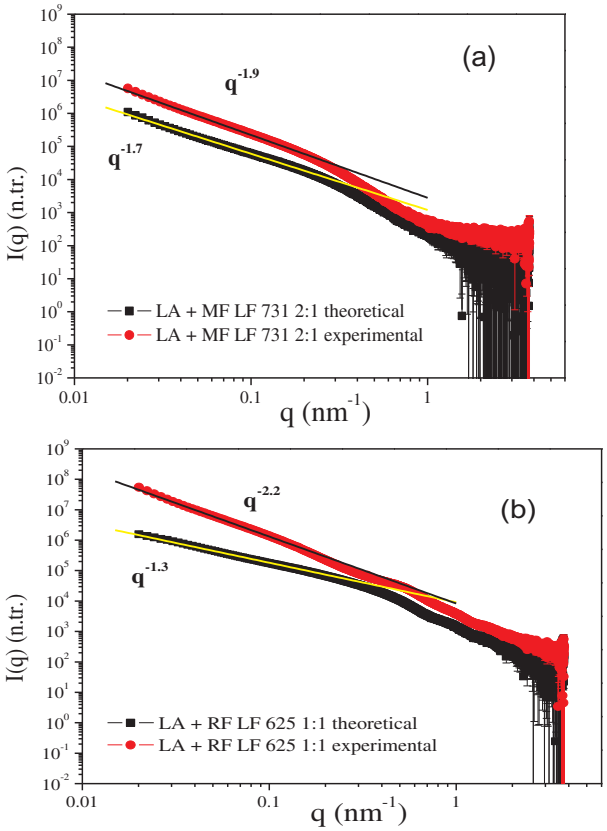

Fig. 2. Theoretical and experimental scattering curves of lysozyme amyloid fibrils in the presence of magnetoferrinin (*a*) and reconstructed ferritin (*b*). Power law fits show mass fractals with dimension D = 1.7 (LA + MF LF 731 theor.), D = 1.9 (LA + MF LF 731 exper.), D = 1.3 (LA + RF LF 625 theor.) and D = 2.2 (LA + RF LF 625 exper.).

same diameter and converted to absolute units using scattering of pure water (program SuperSAXS, by C. L. P. de Oliveira and J. S. Pedersen).

The second set of measurements was performed at the P12 BioSAXS beamline of the European Molecular Biology Laboratory (EMBL) at the storage ring PETRA III of the Deutsche Elektronen Synchrotron (DESY, Hamburg, Germany) with Pilatus 2 M detector (1475 × 1679 pixels, pixel size 172 × 172 μm^2) (Dectris, Switzerland). Synchrotron radiation with a wavelength of 0.1 nm was used. The sample-detector distance was 3 m, allowing measurements in a *q*-range from 0.02 to 3.8 nm^{-1}. The *q*-range was calibrated using the diffraction patterns of silver behenate. The experimental data were normalized to the transmitted beam intensity, corrected for a non-homogeneous detector response, and the background scattering of the aqueous buffer was subtracted. An automatic sample changer for sample volume of 20 μl was used. The experimental time including sample loading, exposure, cleaning and drying was about 1 min per sample. The solvent scattering was measured before and after the sample scattering in order to control the eventual sample holder contamination. Twenty of diffraction patterns were collected for every sample, each with an exposure time of 0.05 s. To avoid radiation damage by subsequent illuminations, scattering curves showing deviations were discarded. The final scattering curve was obtained using the automated acquisition and analysis by averaging the scattering data collected from different frames [33].

Further SAXS data treatment was performed in PRIMUS [34]. Indirect Fourier transformation from reciprocal to real space for construction of pair distance distribution functions *p(r)* (the distribution of distances between all pairs of points within the particle weighted by the respective electron densities [35]) was carried out using GNOM programs [36].

2.6. Atomic force microscopy

Samples for atomic force microscopy (AFM) were prepared by dropping the sample on freshly cleaved pieces of mica (PELCO Mica Sheets Grade V5, 15 × 15 mm^2). After 5–10 min adsorption, the samples were washed with ultrapure water and left to dry at ambient temperature (typically for 1 h). AFM scans were carried out using Agilent 5500 AFM system equipped by PicoView 1.14.3 control software. The topography images were acquired in the tapping mode with standard silicon cantilevers (Olympus, model OMCL-AC 160TS) with resonant frequency 300 kHz, and spring constant 26 N/m. All measurements were carried out at ambient temperature in air, while relative humidity was in the range of 30–40%. Images were processed using freely available software from Gwyddion (http://gwyddion.net).

2.7. Thioflavin T fluorescence assay

Thioflavin T (ThT) is a cationic benzothiazole dye showing enhanced fluorescence upon binding to protein amyloid fibrils. ThT was added to the lysozyme amyloid aggregates and mixtures of lysozyme amyloid aggregates with magnetoferritin or reconstructed ferritin. The final concentrations of ThT and lysozyme aggregates were always 20 μM and 10 μM, respectively. Fluorescence intensities measurements were performed in a 96-well plate by a Synergy MX (BioTek) spectrofluorimeter. The excitation wavelength was set at 440 nm and the emission recorded at 485 nm. The excitation and emission slits were adjusted to 9.0/9.0 nm and the top probe vertical offset was 6 mm. All ThT fluorescence experiments were performed in triplicate and the final value is the mean of measured values.

3. Results and discussion

Magnetoferritin (MF) and reconstructed ferritin (RF) were prepared and analyzed for their possible effect on lysozyme amyloid aggregates. The loading factor values of prepared MF and RF were 731 and 625, respectively, using modified conditions with respect to iron ion and oxidant concentrations. Specific regulation of synthesis conditions allowed us to prepare two types of artificial ferritins: i) MF with magnetite/maghemite iron core [15,16] and ii) RF with ferrihydrite-like iron core [28–30]. Presence of two types of iron minerals inside apoferritin offered the possibility to investigate the effect of magnetic core of different nature and with different magnetization [32] on lysozyme amyloid fibrils. After adding MF or RF into solution containing lysozyme amyloid fibrils, sedimentation was observed, indicating the destruction of amyloids and aggregation of the ferritin proteins. While the supernatant was slightly brown coloured, the sediment containing MF was dark brown. Sedimentation in the RF mixtures was more extensive, with orange coloured sediment. It must be noted that pure initial MF, RF and LA solution did not settle.

To exclude the possible effect of the buffer solutions of MF or RF (AMPSO and HEPES respectively) on the amyloids, the scattering curves of lysozyme amyloid aggregates dispersed in AMPSO and HEPES buffers were measured (Fig. 1a). As expected, the SAXS curves of pure LA in different buffers, similarly to our previous observations, show the presence of large aggregates [31]. Scattering curves of LA dispersed in various buffers with different pH values were compared to determine whether different buffers can alter the structure of lysozyme aggregates. As seen in Fig. 1b, the recorded SAXS curves are almost identical.

The SAXS curve for mixture of LA with pure apoferritin indicates presence of larger objects. The pH value of LA + apoferritin mixture was ~7.5, at which conditions apoferritin is stable, as shown in our previous study [37]. The formation of larger aggregates (agglomerates) is therefore attributed to interactions between LA and apoferritin. SAXS measurements were carried out also for mixtures of MF/RF with LA at amyloid:ferritin weight ratios of 2:1, 1:1, 1:2, 1:5 and 1:10. For comparison with experimental scattering curves of mixtures after

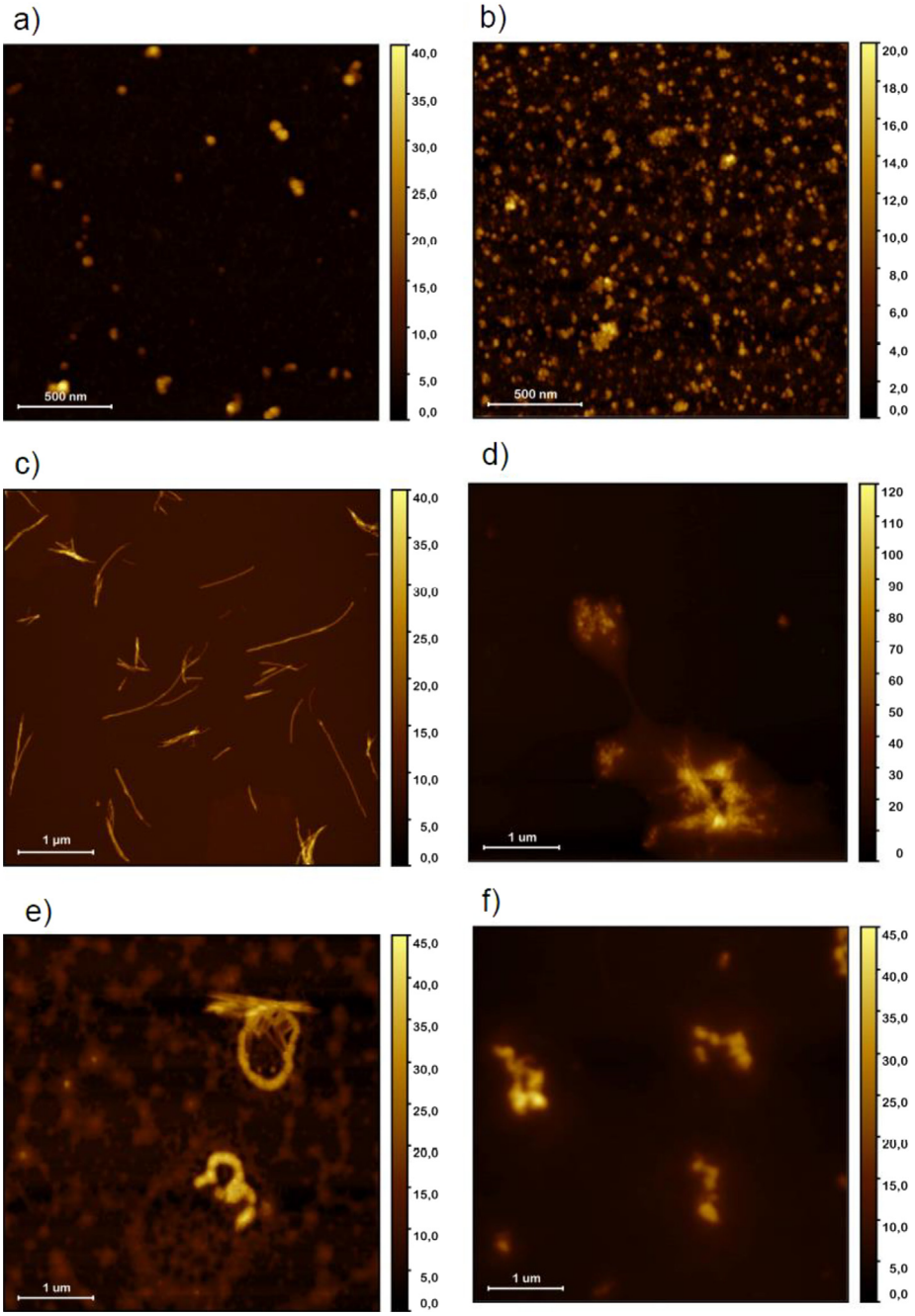

Fig. 3. Atomic force microscopy images of (a) magnetoferritin; (b) reconstructed ferritin; (c) lysozyme amyloid fibrils; (d) mixture of LA + MF 2:1; (e) mixture of LA + MF 1:10; (f) mixture of LA + RF 2:1.

incubation, "theoretical" curves were plotted as well. "Theoretical" curves were calculated as linear combination of the intensities of the two pure initial materials, weighted by the volume fraction ε of the components, according to the equation:

$$I_{(theor)} = \varepsilon_{LA} \times I_{(LA)} + \varepsilon_{(MF/RF)} \times I_{(MF/RF)}.$$

Representative graphs in Fig. 2 shows structural changes happening in the mixed systems, as the difference between the experimental and theoretical curves: the increase of the scattering intensity at low q and the appearance of mass fractals with dimension D = 1.9 and 2.2 for mixture LA + MF and LA + RF, respectively. These results evidence the presence of interactions between MF/RF and LA, leading to reduction of the amount and/or the size of LA.

The pair-distance distribution (PDD) function $p(r)$, containing information about the real space structure of the particles, was constructed (not shown in the manuscript) for initial solutions LA, MF and RF and for mixtures of LA + MF/RF. The p(r) functions were calculated with strong condition of zero at chosen maximal size (which is not the case in present study) and plotted just to show that we have some changes in the structure of our object at length scale up to 100 nm (the shift in position of maximum). The presence of LA in the mixtures leads to a shift in the $p(r)$ maximum to higher r values. The shape of $p(r)$ functions for pure MF and RF indicates the partial shell destruction similar to that observed in our previous works [26,27].

Our SAXS results favour the scenario that interactions between lysozyme amyloid aggregates and magnetoferritin or reconstructed ferritin lead to decrease of both, size and amount of LA. AFM images of pure MF and RF are presented in Fig. 3a and b, respectively. Besides

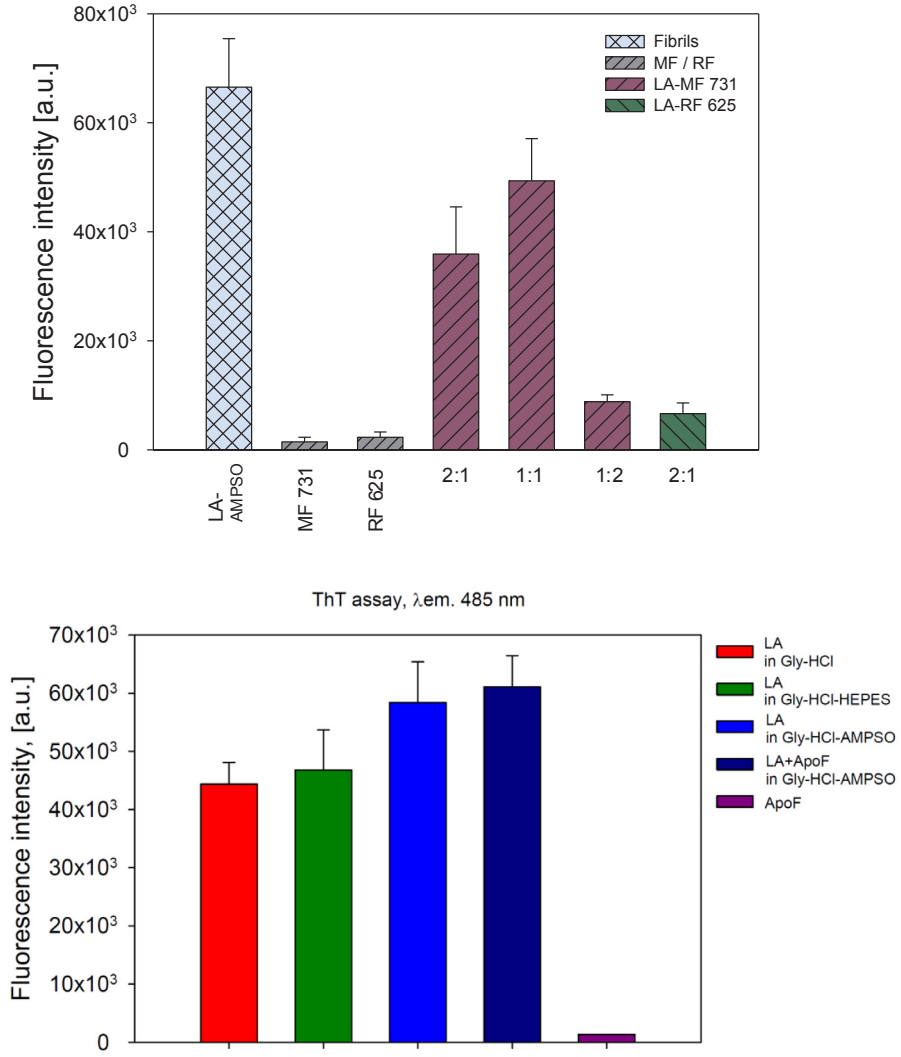

Fig. 4. (a) Effect of magnetoferritin and reconstructed ferritin on lysozyme amyloid aggregates measured using Thioflavin T fluorescence assay. (b) ThT fluorescence intensity in the presence of apoferritin, lysozyme amyloid aggregates (alone) dispersed in various buffers and mixture of LA with apoferritin. Each experiment was performed in triplicate; error bars represent the average deviation for repeated measurements of three separate samples.

single nanoparticles, also particle agglomerates were observed. Typical structure of lysozyme amyloid fibrils is presented in Fig. 3c. Interaction between LA and MF and formation of large agglomerates was observed, as documented in Fig. 3d for mixture at ratio LA:MF 2:1. Similar effect was observed for ratio 1:10 (Fig. 3e) and for mixture LA + RF in ratio 2:1 (Fig. 3f).

Additionally, thioflavin T assay (ThT) was performed to quantify the effect of MF/RF on amount of LA. As ThT fluorescence intensity depends on the amount of amyloid aggregates, no ThT fluorescence intensity was observed in case of native protein as well as for pure MF and RF (Fig. 4a). However, presence of MF or RF, respectively, led to significant decrease of ThT fluorescence intensity suggesting reduction of LA amount. It was shown, that ThT fluorescence intensity of mixtures of LA and MF/RF depends on the relative amount of the components. The significant reduction of amount of LA was observed at weight ratios 1:2 (LA:MF) and 2:1 (LA:RF) most probably caused by presence of iron core with reactive surface capable to destruct LA. In addition, ThT fluorescence intensity was measured for LA dispersed in various buffers to check and exclude possible effect of pH on reduction and changes of LA. The results show a weak influence of pH on the amount of LA. They are stable in various types of buffers and also in the presence of apoferritin.

The results obtained in all three experiments indicate the presence of interaction between both artificial ferritins – magnetoferritin and reconstructed ferritin with lysozyme amyloid aggregates. As an outcome of such interaction, agglomerates (aggregates) formation as well as reduction of the number of LA were observed. Moreover, it seems that the magnetic character of prepared ferritins does not play a significant role, since the destruction effect is observed for both kinds of iron materials inside the apoferritin shell.

4. Conclusion

We studied interactions between lysozyme amyloid fibrils and two types of magnetic materials, magnetoferritin and reconstructed ferritin using small-angle X-ray scattering, atomic force microscopy and fluorescence spectroscopy. Our results show that both magnetoferritin and reconstructed ferritin affect the size, structure and amount of lysozyme amyloid fibrils depending on the mass ratio between these components. Our investigations suggest that the main role can be attributed to the presence of iron, while the magnetic character of both artificial ferritins does not affect destruction of lysozyme amyloid fibrils. It is not excluded that magnetoferritin and reconstructed ferritin could be used in vivo as potential therapeutic agents against amyloid disorders. Previously we have shown that magnetite nanoparticles exhibit anti-amyloidogenic effect in the cerebrospinal fluid of patients with multiple sclerosis and Alzheimer's disease [38]. Although the exact mechanism

of lysozyme amyloid fibrils – magnetoferritin/reconstructed ferritin is not yet known in detail, we believe that the outcome from this work will enable us to aid in designing more effective ferritin derivatives for elucidate the etiology of neurodegenerative diseases and affecting the progression of amyloid-related diseases in vivo.

Acknowledgements

This work was supported by the project of the Slovak Scientific Grant Agency VEGA (project No. 2/0016/17 and No. 2/0062/16), the Slovak Research and Development Agency, Slovakia under the contract No. APVV-015-0453, APVV SK-TW-2017-0012 and by the European Fund of Regional Development (projects No. 26210120012 and No. 26220220186). The authors thank Dr. Franke and Dr. Hajizadeh for the technical assistance during SAXS measurements on P12 beamline at PETRAIII in DESY, Hamburg (Germany).

References

[1] E.H. Koo, P.T. Lansbury Jr, J.W. Kelly, Proc. Natl. Acad. Sci. USA 96 (1999) 9989.
[2] M.F. Perutz, Brain Res. Bull. 50 (1999) 467.
[3] J.Q. Trojanowski, M. Goedert, T. Iwatsubo, V.M. Lee, Cell Death Differ. 5 (1998) 832.
[4] L.S. Itzhaki, P.A. Evans, C.M. Dobson, S.E. Radford, Biochemistry 33 (1994) 5212.
[5] M.R. Krebs, D.K. Wilkins, E.W. Chung, M.C. Pitkeathly, A.K. Chamberlain, J. Zurdo, C.V. Robinson, C.M. Dobson, J. Mol. Biol. 300 (2000) 541.
[6] S. Goda, K. Takano, Y. Yamagata, R. Nagata, H. Akutsu, S. Maki, K. Namba, K. Yutani, Protein Sci. 9 (2000) 369.
[7] A. Cao, D. Hu, L. Lai, Protein Sci. 13 (2004) 319.
[8] J. Geng, M. Li, J. Ren, E. Wang, X. Qu, Angew. Chem. Int. Ed. Engl. 50 (2011) 4184.
[9] M. Mahmoudi, F. Quinlan-Pluck, M.P. Monopoli, S. Sheibani, H. Vali, K.A. Dawson, I. Lynch, ACS Chem. Neurosci. 4 (2013) 475.
[10] R. Mishra, B. Bulic, D. Sellin, S. Jha, H. Waldmann, R. Winter, Angew. Chem. Int. Ed. Engl. 47 (2008) 4679.
[11] S. Linse, C. Cabaleiro-Lago, W.F. Xue, I. Lynch, S. Lindman, E. Thulin, S.E. Radford, K.A. Dawson, Proc. Natl. Acad. Sci. USA 104 (2007) 8691.
[12] A. Bellova, E. Bystrenova, M. Koneracka, P. Kopcansky, F. Valle, N. Tomasovicova, M. Timko, J. Bagelova, F. Biscarini, Z. Gazova, Nanotechnology 21 (2010) 065103.
[13] K. Siposova, M. Kubovcikova, Z. Bednarikova, M. Koneracka, V. Zavisova, A. Antosova, P. Kopcansky, Z. Daxnerova, Z. Gazova, Nanotechnology. 23 (2012) 055101.
[14] K. Siposova, K. Pospiskova, Z. Bednarikova, I. Safarik, M. Safarikova, M. Kubovcikova, P. Kopcansky, Z. Gazova, J. Magn. Magn. Mater. 427 (2017) 48.
[15] K.K.W. Wong, T. Douglas, S. Gider, D.D. Awschalom, S. Mann, Chem. Mater. 10 (1998) 279.
[16] J.W. Bulte, T. Douglas, S. Mann, R.B. Frankel, B.M. Moskowitz, R.A. Brooks, C.D. Baumgarner, J. Vymazal, J.A. Frank, Invest. Radiol. 29 (1994) 214.
[17] F.C. Meldrum, B.R. Heywood, S. Mann, Science 257 (1992) 522.
[18] O. Kasyutich, A. Sarua, W. Schwarzacher, J. Phys. D: Appl. Phys. 41 (2008) 134022.
[19] O. Kasyutich, D. Tatchev, A. Hoell, F. Ogrin, C. Dewhurst, W. Schwarzacher, J. Appl. Phys. 105 (2009) 07B528.
[20] D.P.E. Dickson, S.A. Walton, S. Mann, K. Wong, Nanostruct. Mater. 9 (1997) 595.
[21] Q.A. Pankhurst, S. Betteridge, D.P.E. Dickson, T. Douglas, S. Mann, R.B. Frankel, Hyperfine Interact. 91 (1994) 847.
[22] M.J. Martínez-Pérez, R. de Miguel, C. Carbonera, M. Martínez-Júlvez, A. Lostao, C. Piquer, C. Gómez-Moreno, J. Bartolomé, F. Luis, Nanotechnology 21 (2010) 465707.
[23] F. Moro, R. de Miguel, M. Jenkins, C. Gómez-Moreno, D. Sells, F. Tuna, E.J.L. McInnes, A. Lostao, F. Luis, J. van Slageren, J. Magn. Magn. Mater. 361 (2014) 188.
[24] M. Koralewski, M. Pochylski, Z. Mitróová, M. Timko, P. Kopčanský, L. Melníková, J. Magn. Magn. Mater. 323 (2011) 2413.
[25] M. Koralewski, J.W. Kłos, M. Baranowski, Z. Mitroova, P. Kopcansky, L. Melnikova, M. Okuda, W. Schwarzacher, Nanotechnology 23 (2012) 355704.
[26] L. Melníková, V.I. Petrenko, M.V. Avdeev, V.M. Garamus, L. Almásy, O.I. Ivankov, L.A. Bulavin, Z. Mitróová, P. Kopčanský, Coll. Surf. B. 123 (2014) 82.
[27] L. Melnikova, V.I. Petrenko, M.V. Avdeev, O.I. Ivankov, L.A. Bulavin, V.M. Garamus, L. Almásy, Z. Mitroova, P. Kopcansky, J. Magn. Magn. Mater. 377 (2015) 77.
[28] I.G. Macara, T.G. Hoy, P.M. Harrison, Biochem. J. 126 (1972) 151.
[29] S. Levi, A. Luzzago, G. Cesareni, A. Cozzi, F. Franceschinelli, A. Albertini, P. Arosio, J. Biol. Chem. 263 (1988) 18086.
[30] S. Sun, N.D. Chasteen, J. Biol. Chem. 267 (1992) 25160.
[31] P. Kopcansky, K. Siposova, L. Melnikova, Z. Bednarikova, M. Timko, Z. Mitroova, A. Antosova, V.M. Garamus, V.I. Petrenko, M.V. Avdeev, J. Magn. Magn. Mater. 377 (2015) 267.
[32] Z. Mitróová, L. Melníková, J. Kováč, M. Timko, P. Kopčanský, Acta Phys. Pol. A 121 (2012) 1318.
[33] D. Franke, A.G. Kikhney, D.I. Svergun, Nucl. Instrum. Methods A 689 (2012) 52.
[34] P.V. Konarev, V.V. Volkov, A.V. Sokolova, M.H.J. Koch, D.I. Svergun, J. Appl. Cryst. 36 (2003) 1277.
[35] D.I. Svergun, M.H.J. Koch, Rep. Prog. Phys. 66 (2003) 1735.
[36] D.I. Svergun, J. Appl. Crystallogr. 25 (1992) 495.
[37] L. Balejčíková, V.M. Garamus, M.V. Avdeev, V.I. Petrenko, L. Almásy, P. Kopčanský, Colloids Surf. B Biointerfaces. 156 (2017) 375.
[38] Z. Kristofikova, Z. Gazova, K. Siposova, A. Bartos, J. Ricny, J. Kotoucova, J. Sirova, D. Ripova, Neurochem. Res 39 (2014) 391502.